

# Relation of Insulin Resistance to Longitudinal Changes in Left Ventricular Structure and Function in a General Population

Nicholas Cauwenberghs, MSc; Judita Knez, MD, PhD; Lutgarde Thijs, MSc; Francois Haddad, MD; Thomas Vanassche, MD, PhD; Wen-Yi Yang, MD; Fang-Fei Wei, MD; Jan A. Staessen, MD, PhD; Tatiana Kuznetsova, MD, PhD

**Background**—Population data on the longitudinal changes of left ventricular (LV) structure and function in relation to insulin resistance are sparse. Therefore, we assessed in a general population whether hyperinsulinemia predicts longitudinal changes in LV and arterial characteristics.

**Methods and Results**—In 627 participants (mean age 50.7 years, 51.4% women), we assessed echocardiographic indexes of LV structure and function and carotid-femoral pulse wave velocity by applanation tonometry at baseline and after 4.7 years. We regressed longitudinal changes in these indexes on baseline insulin and its change during follow-up, and reported standardized effect sizes as a percentage of the SD of LV changes associated with a doubling of insulin. After adjustment, higher baseline insulin predicted a greater temporal increase in LV mass index (effect size: +15.1%) and E/e' ratio (+22.1%), and a greater decrease in e' peak and longitudinal strain (−11.2% to −17.1%). A greater increase in insulin during follow-up related to a greater increase in LV mass index (+10.7%) and decline in ejection fraction and longitudinal strain (−11.4% to −15.7%). Participants who became or remained insulin resistant during follow-up experienced worse changes in longitudinal strain, E/e', and LV mass index as compared with participants who did not develop or had improved insulin resistance over time ( $P \leq 0.033$ ). Moreover, multivariable-adjusted increase in pulse wave velocity was higher in participants with diabetes mellitus than in participants without diabetes mellitus (+1.46 m/s versus +0.71 m/s;  $P = 0.039$ ).

**Conclusions**—Hyperinsulinemia at baseline and during follow-up predicted worsening of LV function and remodeling over time. Our findings underline the importance of management of insulin resistance. (*J Am Heart Assoc.* 2018;7:e008315. DOI: 10.1161/JAHA.117.008315.)

**Key Words:** arterial stiffness • insulin resistance • left ventricular function • longitudinal strain • population studies

Diabetes mellitus is a surging contributor to the epidemic of heart failure (HF).<sup>1</sup> In patients with symptomatic HF, the presence of diabetes mellitus independently increases the

risk of cardiovascular outcomes such as HF hospitalization rates and mortality.<sup>2,3</sup> As the process of adverse myocardial remodeling and dysfunction starts years to decades before the onset of HF symptoms, recent guidelines emphasized the timely identification and management of risk factors for HF such as hypertension, obesity, and diabetes mellitus.<sup>4</sup>

Within this context, insulin resistance may play an important role in the initiation and progression of metabolic cardiomyopathy. Numerous experimental studies have already demonstrated a cluster of disturbances in cell metabolism and signaling induced by insulin resistance that adversely affects left ventricular (LV) contractility and stiffness.<sup>5–7</sup> For instance, in the stressed state (eg, ischemia, pressure load, injury), the impaired ability of the insulin-resistant cardiomyocytes to switch from free fatty acid (FFA) to more effective glucose oxidation metabolism limits the heart's capacity for adaptive energy response.<sup>7</sup> The compensatory augmentation of FFA metabolism, in turn, leads to increased oxygen consumption, decreased cardiac efficiency, and lipotoxicity.<sup>8</sup> It was also established that metabolic disturbances triggered by hyperglycemia, insulin resistance, and increased FFA levels induce

From the Research Unit Hypertension and Cardiovascular Epidemiology (N.C., L.T., W.-Y.Y., F.-F.W., J.A.S., T.K.) and Centre for Molecular and Vascular Biology (T.V.), KU Leuven Department of Cardiovascular Sciences, University of Leuven, Belgium; Division of Internal Medicine, Department of Hypertension, University Medical Centre Ljubljana, Slovenia (J.K.); Stanford Cardiovascular Institute, Stanford, CA (F.H.).

Accompanying Data S1, Tables S1 through S6, and Figures S1 and S2 are available at <http://jaha.ahajournals.org/content/7/7/e008315/DC1/embed/inline-supplementary-material-1.pdf>

**Correspondence to:** Tatiana Kuznetsova, MD, PhD, Research Unit of Hypertension and Cardiovascular Epidemiology, KU Leuven Department of Cardiovascular Sciences, University of Leuven, Campus Sint Rafaël, Kapucijnenvoer 35, Box 7001, B-3000 Leuven, Belgium. E-mail: [tatiana.kouznetsova@med.kuleuven.be](mailto:tatiana.kouznetsova@med.kuleuven.be)

Received December 8, 2017; accepted February 14, 2018.

© 2018 The Authors. Published on behalf of the American Heart Association, Inc., by Wiley. This is an open access article under the terms of the Creative Commons Attribution-NonCommercial License, which permits use, distribution and reproduction in any medium, provided the original work is properly cited and is not used for commercial purposes.

## Clinical Perspective

### What Is New?

- In this longitudinal population study, we showed that higher levels of insulin at baseline and its increase over follow-up were associated with the decline in left ventricular systolic performance (by longitudinal strain and ejection fraction), worsening of diastolic function (by  $E/e'$ ), and increase in left ventricular mass index.

### What Are the Clinical Implications?

- Effective management of insulin resistance may prevent or delay the development of adverse left ventricular remodeling and dysfunction preceding metabolic cardiomyopathy and symptomatic heart failure.
- The preventive strategies might tackle the rising contribution of (pre)diabetes mellitus to the epidemic of symptomatic heart failure.

oxidative stress and chronic low-grade inflammation, which leads to microvasculopathy and macrovasculopathy.<sup>9</sup>

Previous cross-sectional large-scale community-based studies have demonstrated an independent association of subclinical LV remodeling and dysfunction with insulin resistance.<sup>10–15</sup> On the other hand, population data on the longitudinal changes of LV structure and function in relation to insulin resistance are sparse. Serial imaging studies are essential to elucidate the impact of insulin resistance on early signs of LV maladaptation and arterial stiffness that forerun symptomatic HF and other cardiovascular outcomes. Therefore, in a general population sample, we prospectively tested the hypothesis that hyperinsulinemia and insulin resistance predict alterations in echocardiographic indexes of LV structure and function and arterial stiffness over time.

## Methods

The data, analytic methods, and study materials will be made available to other researchers for purposes of reproducing the results or replicating the procedure. Because consent given by study participants did not include data sharing with third parties, anonymized data can be made available to investigators for analysis on reasonable request to the corresponding author.

## Study Participants

The ethics committee of the University of Leuven approved the FLEMENGHO (Flemish Study on Environment, Genes and Health Outcomes). From 1985 until 2005, we randomly recruited a family-based population sample within a

geographically defined area in northern Belgium as described elsewhere.<sup>16</sup> From 2005 to 2009, we invited 1031 former participants for an examination including echocardiography and applanation tonometry. We obtained written informed consent in 828 participants (participation rate, 80.3%). We invited these participants for a follow-up examination on average 4.7 years (5th–95th percentile, 3.7–5.4 years) after their first echocardiographic examination. We excluded 147 participants because they died ( $n=25$ ), were lost to follow-up ( $n=19$ ), or declined the follow-up invitation ( $n=103$ ). For this analysis, we additionally excluded 54 participants presenting with atrial fibrillation ( $n=12$ ), an artificial pacemaker ( $n=4$ ), or insufficient echocardiographic image quality ( $n=38$ ) at baseline and/or at follow-up. In total, we statistically analyzed 627 participants (Figure S1).

## Echocardiography

### Data acquisition

A detailed echocardiographic protocol is provided in Data S1. Briefly, an experienced physician (T.K.) performed both echocardiographic examinations using a Vivid7 Pro and Vivid E9 (GE Vingmed), respectively, interfaced with a 2.5- to 3.5-MHz phased-array probe.<sup>16,17</sup> With the participants in partial left decubitus, the observer obtained images along the parasternal long and short axes and from the apical 4- and 2-chamber and long-axis views together with a simultaneous ECG signal.

### Offline analysis

One observer (T.K.) analyzed the digitally stored echocardiograms blinded to the participants' characteristics using EchoPac software (GE Vingmed). Measurements were averaged over 3 heart cycles for statistical analysis. LV internal diameter and interventricular septal and posterior wall thickness were measured from the 2-dimensionally guided M-mode tracing at end-diastole. Relative wall thickness was calculated as  $0.5 \times (\text{interventricular septum} + \text{posterior wall}) / \text{LV internal diameter at end-diastole}$ . End-diastolic LV dimensions were used to calculate LV mass. Using the standard Simpson method, LV volumes and ejection fraction (EF) were derived from the apical 4- and 2-chamber views. Transmitral blood flow signals were used to measure peak early (E) and late (A) diastolic velocity and E/A ratio. From pulsed-wave tissue Doppler imaging (TDI) recordings, we measured the peak systolic ( $s'$ ) and early diastolic ( $e'$ ) velocities of the mitral annulus at septal, lateral, inferior, and posterior acquisition sites.  $E/e'$  ratio was calculated by dividing transmitral E peak by  $e'$  averaged from the 4 acquisition sites.

As previously described,<sup>16</sup> 2 observers (T.K., N.C.) derived LV longitudinal strain (LS) using commercially available

myocardial speckle-tracking software (Q-analysis, GE Vingmed) at default settings. The LV endocardial border was manually traced at the end-systolic frame of the 2-dimensional 4-chamber view. The software automatically tracked myocardial speckle motion while dividing the region of interest in LV basal, mid, and apical levels. We adjusted the region of interest after visual evaluation of the tracking. Images were rejected if tracking was inadequate in  $\geq 2$  segments. We obtained basal-mid and apical LS by averaging the segmental LS of the respective regions. We used absolute values of peak systolic midwall LS for statistical analysis. Detailed information on interobserver reproducibility of LS is provided in Data S1.

## Arterial Stiffness

Arterial tonometry was performed using an SPC-301 micro-manometer (Millar Instruments Inc.) interfaced with a laptop running SphygmoCor version 7.1 (AtCor Medical Pty Ltd).<sup>18</sup> At baseline and follow-up, trained observers successfully recorded ECG-gated arterial pressure waveforms in both the carotid and femoral arteries in 420 participants. We measured the distance from the suprasternal notch to the carotid sampling site and from the suprasternal notch to the femoral sampling site. Pulse transit time was the time between the upstroke of carotid and femoral pulse averaged for 10 consecutive beats. Aortic pulse wave velocity (PWV), the current noninvasive gold standard of arterial stiffness,<sup>18</sup> was the ratio of the carotid-sternal-femoral distance (in meters) to the pulse transit time (in seconds). Intraobserver intrasession reproducibility was 2.61%.

## Other Measurements

Conventional blood pressure was the average of 5 auscultatory readings obtained with the patient in the seated position. Hypertension was defined as a blood pressure of at least 140 mm Hg systolic or 90 mm Hg diastolic and/or the use of antihypertensive drugs. We administered a standardized questionnaire to collect detailed information on medical history, lifestyle, and intake of medications. Fasting venous blood samples were drawn for measurement of biomarkers. Baseline and follow-up serum insulin levels were measured by an Elecsys sandwich immunoassay (Roche Diagnostics). Diabetes mellitus was determined by self-report, a fasting glucose level of at least 126 mg/dL, or the use of antidiabetic agents. We calculated the Homeostatic Model Assessment of Insulin Resistance (HOMA-IR) as the product of fasting glucose (in mmol/L) and serum insulin (in  $\mu\text{mol/L}$ ) divided by 22.5. Participants whose HOMA-IR values exceeded the 75th percentile (ie, 2.62) were considered to have insulin resistance.<sup>19</sup>

## Statistical Analysis

For database management and statistical analysis, we used SAS version 9.4 (SAS Institute). We compared means and proportions between baseline and follow-up visits by a paired *t* test and McNemar test, respectively. Significance was  $P < 0.05$  on 2-sided tests. We checked the distributions of all biochemical parameters and normalized them by a logarithmic transformation if needed.

By use of a mixed model, we assessed multivariable-adjusted associations between longitudinal changes in echocardiographic LV indexes and serum insulin levels while accounting for family clusters. All models were adjusted for baseline LV index, follow-up duration, age, sex, heart rate, body height, body weight, pulse pressure, and mean arterial pressure, as well as longitudinal changes in these risk factors.<sup>20,21</sup> Our models were also adjusted for starting, remaining, or stopping antihypertensive treatment (per drug class, if needed). We reported the multivariable-adjusted regression coefficients per doubling in serum insulin and its percentage of longitudinal change on a relative scale as a percentage of the standardized effect size (ie, the absolute effect size divided by the SD of the echocardiographic changes multiplied by 100). We also expressed adjusted regression coefficients for LV changes in each quartile of HOMA-IR relative to the overall LV change in the whole study population, which allowed quartile-specific computation of regression coefficients without definition of an arbitrary reference group.

Next, we constructed a partial regression diagram including multivariable-adjusted changes in LV phenotype and serum insulin using JMP Genomics 6.0. This approach fits covariance selection models, estimating the correlation between pairs of variables adjusted for their correlations with all other variables in the network (ie, partial correlations). In contrast to the 1-to-1 associations retrieved from the mixed models, this method provides adjusted correlations while accounting for the complex relations of the LV structural and functional indexes with one another.

Finally, we performed forward stepwise regression to determine clinical correlates of changes over time in PWV. Covariables considered in stepwise regression were baseline PWV, years of follow-up, age, sex, body mass index, heart rate, pulse pressure, mean arterial pressure, smoking, history of diabetes mellitus, history of coronary heart disease, serum creatinine, total cholesterol, blood sugar, serum insulin, HOMA-IR, and starting, remaining, or stopping antihypertensive treatment (per drug class). We also included longitudinal changes in these risk factors in the stepwise models. We set the *P* value for variables to enter the stepwise regression models at 0.15 and selected variables with  $P < 0.05$ .

**Table 1.** Clinical Characteristics of 627 Participants at Baseline and Follow-Up Examination

Characteristic	Visit 1 (2005–2009)	Visit 2 (2009–2013)	$\Delta$	P Value
<b>Anthropometrics</b>				
Age, y	50.6±14.6	55.3±14.5	+4.72±0.58	<0.0001
Body mass index, kg/m <sup>2</sup>	26.4±4.14	27.1±4.19	+0.71±1.85	<0.0001
Waist circumference, cm	89.9±12.0	95.3±12.2	+5.36±7.31	<0.0001
Brachial systolic BP, mm Hg	128.6±16.7	132.1±16.8	+3.52±13.5	<0.0001
Brachial diastolic BP, mm Hg	79.8±9.38	82.2±9.73	+2.45±8.63	<0.0001
Brachial pulse pressure, mm Hg	48.8±14.2	49.9±15.6	+1.07±11.3	0.017
Mean arterial pressure, mm Hg	96.0±10.4	98.8±10.2	+2.81±9.08	<0.0001
Heart rate, beats per min	60.3±9.35	60.0±9.63	−0.32±7.47	0.29
<b>Questionnaire data, No. (%)</b>				
Current smoking	121 (19.3)	98 (15.6)	−3.7%	<0.0001
Drinking alcohol	259 (41.3)	239 (38.1)	−3.2%	0.072
Hypertensive	259 (41.3)	316 (50.4)	+9.1%	<0.0001
Treated for hypertension	154 (24.6)	203 (32.4)	+7.8%	<0.0001
β-Blockers	94 (15)	107 (17.1)	+2.1%	0.066
ACEIs or ARBs	51 (8.14)	86 (13.7)	+5.6%	<0.0001
CCBs or α-blockers	26 (4.20)	55 (8.80)	+4.6%	<0.0001
Diuretics	55 (8.77)	69 (11.0)	+2.2%	0.054
History of CHD	22 (3.51)	44 (7.02)	+3.5%	<0.0001
History of diabetes mellitus	21 (3.35)	48 (7.66)	+4.3%	<0.0001
<b>Biochemical data</b>				
Serum creatinine, μmol/L	86.1±15.5	89.6±22.8	+3.47±14.1	<0.0001
Total cholesterol, mmol/L	5.27±0.95	5.02±0.95	−0.25±0.90	<0.0001
hs-CRP, mg/L	1.50 (0.69–5.02)	1.49 (0.63–4.81)	−0.001 (−2.33 to 1.94)	0.99
hs-IL6, pg/mL	1.46 (0.69–3.23)	1.49 (0.70–3.47)	−0.050 (−1.18 to 1.37)	0.80
Blood glucose, mmol/L	4.92±0.73	4.91±0.72	−0.005±0.83	0.89
Serum insulin, μmol/L	4.72 (2.00–10.0)	5.13 (2.00–12.0)	+1.09 (−0.57 to 2.03)	0.0010
HOMA-IR	1.06 (0.13–6.94)	1.28 (0.17–10.2)	+1.21 (−0.23 to 6.78)	0.0042

Values are mean (±SD), number of participants (percentage), or median (10–90% percentile interval). For longitudinal changes ( $\Delta$ ), values are mean (±SD) or geometric mean (10–90% percentile interval) or percentage change. ACEIs indicates angiotensin-converting enzyme inhibitors; ARBs, angiotensin receptor blockers; BP, blood pressure; CCBs, calcium channel blockers; CHD, coronary heart disease; HOMA-IR, Homeostatic Model Assessment of Insulin Resistance; hs-CRP, high-sensitivity C-reactive protein; hs-IL6, high-sensitivity interleukin 6.

## Results

### Characteristics of Participants

At baseline, the mean age of the 627 participants (50.7% women) was 50.6±14.6 years. Tables 1 and 2 present the clinical, PWV, and echocardiographic characteristics of the study cohort by examination phase. Of note, serum insulin increased significantly over time ( $P=0.0010$ ), whereas fasting blood glucose did not significantly change ( $P=0.89$ ; Table 1). Hence, HOMA-IR also increased during follow-up ( $P=0.0042$ ).

From visit 1 to 2, relative wall thickness and LV mass index (LVMI) increased ( $P<0.0001$ ) following an increase in LV wall thicknesses ( $P<0.0001$ ) and decrease in LV internal diastolic

dimensions ( $P=0.030$ ; Table 2). Of LV systolic indexes, EF and TDI  $s'$  peak as well as 4-chamber global and apical LS decreased significantly over time ( $P\leq 0.034$ ). During follow-up, transmitral and TDI  $e'$  and  $a'$  as well as E/A ratio decreased ( $P<0.0001$ ), whereas E/ $e'$  ratio increased ( $P<0.0001$ ).

Tables S1 and S2 show these characteristics by sex and examination phase.

### Associations Between Changes in LV Indexes and Serum Insulin

Table 3 shows the standardized multivariable-adjusted estimates (95% confidence interval) of longitudinal changes in

**Table 2.** PWV and Echocardiographic Characteristics of 627 Patients at Baseline and Follow-Up Examination

Characteristic	Visit 1 (2005–2009)	Visit 2 (2009–2013)	Δ	P Value
PWV,* m/s	7.59±1.71	8.33±2.07	+0.74±1.39	<0.0001
LV structure				
Internal diameter, cm	5.05±0.45	5.03±0.43	−0.026±0.30	0.030
Septal wall, cm	0.98±0.16	1.00±0.16	+0.030±0.12	<0.0001
Posterior wall, cm	0.89±0.14	0.94±0.12	+0.054±0.11	<0.0001
Relative wall thickness, cm	0.37±0.06	0.39±0.05	+0.018±0.05	<0.0001
Mass index, g/m <sup>2</sup>	92.0±20.8	95.6±21.2	+3.72±12.9	<0.0001
Length, cm	8.12±0.75	8.11±0.72	−0.014±0.52	0.50
Δ EDV, mL	99.9±25.6	94.7±25.1	−4.86±17.2	<0.0001
Δ ESV, mL	37.4±11.7	36.9±11.6	−0.40±8.72	0.28
LV systolic function				
Ejection fraction, %	63.5±6.43	61.2±6.43	−2.33±8.21	<0.0001
TDI s' peak, cm/s <sup>‡</sup>	9.08±1.41	8.02±1.30	−1.06±1.04	<0.0001
Global LS, % <sup>†</sup>	19.7±2.36	19.5±2.36	−0.20±2.32	0.034
Basal-mid LS, % <sup>†</sup>	18.5±2.26	18.6±2.18	+0.10±2.15	0.24
Apical LS, % <sup>†</sup>	23.5±4.23	22.0±3.79	−1.44±4.36	<0.0001
LV diastolic function				
Left atrial volume index, mL/m <sup>2</sup>	23.0±6.06	25.8±6.64	+2.87±4.18	<0.0001
E peak, cm/s	75.9±16.0	67.1±15.7	−8.85±11.6	<0.0001
A peak, cm/s	64.6±16.9	60.1±15.1	−3.68±9.15	<0.0001
E/A ratio	1.27±0.47	1.18±0.45	−0.08±0.27	<0.0001
TDI e' peak, cm/s <sup>‡</sup>	11.5±3.56	9.81±3.36	−1.69±1.56	<0.0001
TDI a' peak, cm/s <sup>‡</sup>	10.2±2.06	9.57±2.11	−0.60±1.52	<0.0001
E/e' ratio <sup>‡</sup>	7.04±2.12	7.39±2.45	+0.35±1.43	<0.0001

Values are mean (±SD). For longitudinal changes (Δ), values are mean (±SD). EDV indicates end-diastolic volume; ESV, end-systolic volume; LV, left ventricular; TDI, tissue Doppler imaging.

\*Measurements of pulse wave velocity (PWV) were available at both baseline and follow-up in 420 patients.

<sup>†</sup>Longitudinal strain (LS) measured in the apical 4-chamber view.

<sup>‡</sup>Average of septal, lateral, inferior, and posterior mitral annulus sites.

LV indexes associated with a doubling in serum insulin at baseline or with a doubling of the percentage increase in serum insulin during follow-up. After adjustment, a higher level of serum insulin at baseline predicted a greater temporal increase in LVMI (standardized effect size: +15.1%,  $P=0.0015$ ) and decrease in 4-chamber global LS (−13.5%,  $P=0.0058$ ) and basal-mid LS (−17.1%,  $P=0.0003$  [Table 3]). Moreover, the decrease in TDI e' peak (−11.2%,  $P=0.040$ ) and the increase in E/e' ratio (+22.1%;  $P=0.0002$ ) over time were independently related to higher insulin at baseline. In parallel, we observed that a greater increase in insulin during follow-up was independently associated with a greater increase in LVMI (+10.7%,  $P=0.023$ ) and stronger decline in EF (−11.4%,  $P=0.0028$ ), 4-chamber LS (−12.6%,  $P=0.0033$ ), and basal-mid LS (−15.7%,  $P=0.0001$  [Table 3]). In a sensitivity analysis including 606 participants free from

diabetes mellitus at baseline, these findings remained similar (Table S3).

With exception of changes in posterior wall thickness (+9.97%,  $P=0.011$ ), none of the longitudinal changes in LV structure and function were independently associated with fasting blood glucose at baseline or the changes in blood glucose during follow-up after adjustment including insulin ( $P\geq 0.074$ ; Table S4). Similar to our findings on insulin, higher HOMA-IR at baseline and longitudinal increase in HOMA-IR over time independently predicted a greater increase in LVMI ( $P\leq 0.018$ ) and decrease in EF and 4-chamber LS during follow-up ( $P\leq 0.027$ ; Table S4). Furthermore, a greater longitudinal increase in E/e' ratio was associated with a higher baseline HOMA-IR (+8.85%,  $P=0.0002$ ).

Of the systemic inflammatory markers, change in high-sensitivity C-reactive protein was independently related to



**Table 3.** Multivariable-Adjusted Associations of 4.7 Years of Changes in LV Structure and Function With Serum Insulin

	Baseline Serum Insulin, Per Doubling		$\Delta$ Serum Insulin, Per Doubling of the Percentage Increase	
	Parameter Estimate (95% CI)	P Value	Parameter Estimate (95% CI)	P Value
LV structure				
$\Delta$ Internal diameter, cm	−0.38% (−10.3 to 9.55)	0.94	0.21% (−8.82 to 9.25)	0.96
$\Delta$ Septal wall, cm	3.05% (−6.60 to 12.8)	0.53	5.75% (−3.05 to 14.5)	0.20
$\Delta$ Posterior wall, cm	10.4% (1.90 to 18.9)	0.017	3.00% (−4.69 to 10.8)	0.44
$\Delta$ Relative wall thickness	6.72% (−2.90 to 16.4)	0.17	4.97% (−3.79 to 13.7)	0.27
$\Delta$ Mass index, g/m <sup>2</sup>	15.1% (5.84 to 24.5)	0.0015	10.7% (1.46 to 20.0)	0.023
$\Delta$ EDV, mL	−2.20% (−12.6 to 8.15)	0.68	−4.46% (−13.9 to 4.97)	0.35
$\Delta$ ESV, mL	5.12% (−5.13 to 15.4)	0.33	8.04% (−1.31 to 17.4)	0.092
LV systolic function				
$\Delta$ EF, %	−8.44% (−17.0 to 0.078)	0.052	−11.4% (−18.9 to −5.16)	0.0028
$\Delta$ Global LS, %	−13.5% (−23.1 to −3.94)	0.0058	−12.6% (−20.9 to −4.20)	0.0033
$\Delta$ Basal-mid LS, %	−17.1% (−26.2 to −7.98)	0.0003	−15.7% (−23.6 to −7.77)	0.0001
$\Delta$ Apical LS, %	−4.72% (−13.5 to 4.04)	0.29	−4.83% (−11.8 to 2.84)	0.22
LV diastolic function				
$\Delta$ E peak, cm/s	6.78% (−3.04 to 16.6)	0.18	−2.02% (−10.9 to 6.89)	0.66
$\Delta$ E/A	1.72% (−7.80 to 11.2)	0.72	−6.84% (−15.4 to 2.10)	0.11
$\Delta$ TDI e' peak, cm/s	−11.2% (−22.0 to −0.50)	0.040	−9.34% (−19.0 to 0.33)	0.058
$\Delta$ E/e'	22.1% (10.5 to 33.6)	0.0002	7.56% (−2.89 to 18.0)	0.16

Parameter estimates (95% confidence interval [CI]) are the changes in the left ventricular (LV) indices associated with a doubling of the baseline insulin (second column) or a doubling of the longitudinal percentage increase in insulin (fourth column). The parameter estimates are expressed as a percentage of SD of the longitudinal change ( $\Delta$ ) in LV index. Analyses were adjusted for follow-up duration, baseline LV index, age, sex, heart rate, body height, body weight, pulse pressure, and mean arterial pressure. We additionally adjusted for longitudinal changes in these risk factors and for 3 indicator variables coding for antihypertensive drug class intake (starting or stopping treatment between baseline and follow-up and remaining on treatment). All covariables were identified based on stepwise regression analyses. For LV mass index, models did not include anthropometric characteristics. EDV indicates end-diastolic volume; EF, ejection fraction; ESV, end-systolic volume; LS, longitudinal strain; TDI, tissue Doppler imaging.

higher baseline insulin (+17.1%,  $P=0.0021$ ) and change in insulin (+16.4%,  $P=0.0006$ ). Similarly, high-sensitivity interleukin 6 also increased over time with higher baseline insulin (+14.8%,  $P=0.011$ ). However, the associations of changes in LV indexes with the baseline inflammatory markers and their changes over time did not reach statistical significance after adjustment ( $P\geq 0.078$ ).

### LV Changes in Relation to Progression of Insulin Resistance Status

We further assessed temporal changes in LV 4-chamber LS, E/e' ratio, and LVMI by baseline HOMA-IR quartile (Figure 1) and by progression of insulin resistance status during follow-up (Figure 2 and Table S5). Compared with the averaged LV changes in the whole cohort, participants belonging to the fourth quartile of baseline HOMA-IR distribution (with insulin resistance) experienced more detrimental changes in 4-chamber LS measured at basal-mid segments, E/e' ratio, and LVMI during follow-up ( $P\leq 0.034$ ; Figure 1). Participants

who developed insulin resistance over time ( $n=97$ ) showed a stronger decrease in 4-chamber LS and increase in E/e' ratio compared with those who had normal HOMA-IR ( $n=374$ ) at baseline and during follow-up ( $P\leq 0.018$ ; Figure 2). On the other hand, participants with sustained insulin resistance over time ( $n=94$ ) exhibited worse changes in 4-chamber LS, E/e' ratio, and LVMI as compared with participants with normal HOMA-IR at both visits ( $P\leq 0.026$ ; Figure 2).

### Serum Insulin Within the Network of LV Changes

Figure 3 illustrates a complex network of interactions between the multivariable-adjusted temporal changes in echocardiographic indexes of LV systolic and diastolic function and LV structure. While accounting for these LV traits interactions, the partial regression analysis confirmed the direct relation of higher insulin level at baseline with an increase in LVMI and E/e' during follow-up (Figure 3). Of the LV systolic function indexes, a greater decline in 4-chamber

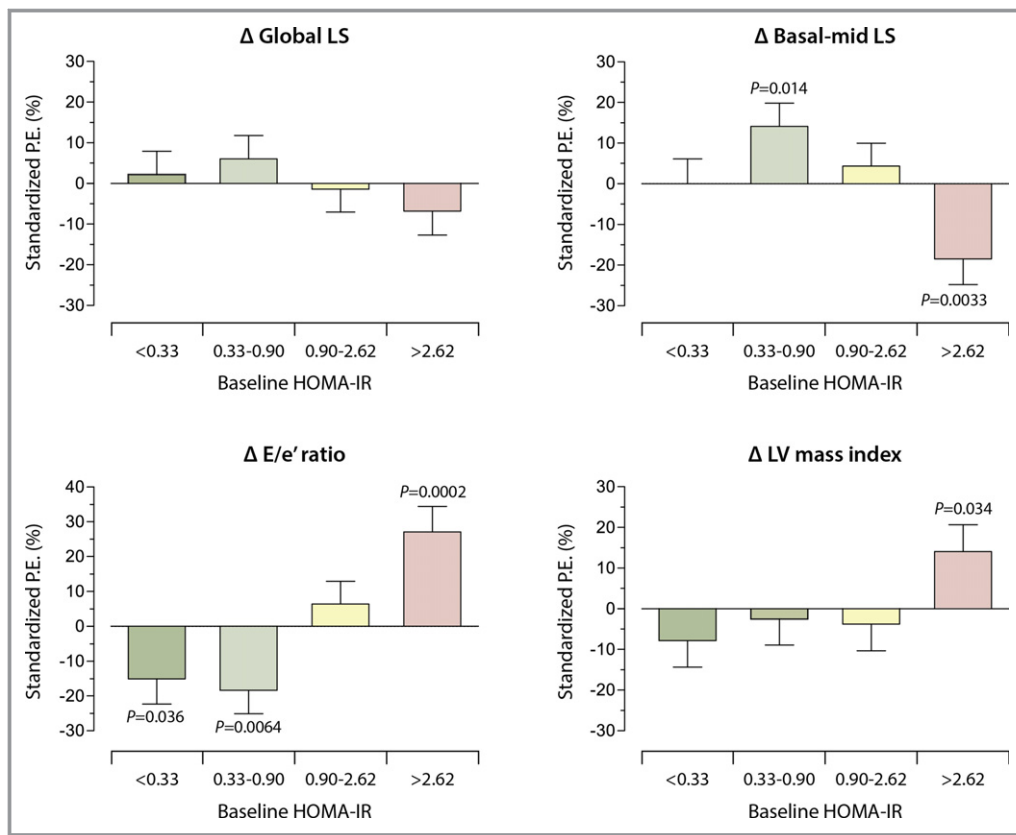


**Figure 1.** Multivariable-adjusted parameter estimates (PEs;  $\pm$ SE) for 4.7 years of change ( $\Delta$ ) in left ventricular (LV) longitudinal strain (LS), E/e', and LV mass index per Homeostatic Model Assessment of Insulin Resistance (HOMA-IR) quartile. Number of participants per quartile: quartile 1,  $n=160$ ; quartile 2,  $n=152$ ; quartile 3,  $n=159$ ; quartile 4:  $n=156$ . Adjusted PEs are expressed as percentage of SD of the longitudinal change in LV index.  $P$  values are for comparisons with the overall LV index changes in the whole cohort. Analyses were adjusted for follow-up duration, baseline LV index, age, sex, heart rate, body height, body weight, pulse pressure, and mean arterial pressure. We additionally adjusted for longitudinal changes in these risk factors and for 3 indicator variables coding for antihypertensive drug class intake (starting or stopping treatment between baseline and follow-up and remaining on treatment).

basal-mid LS remained related to higher insulin level at baseline and its change over time (Figure 3).

Partial regression analysis also confirmed the direct relation of baseline insulin and its change with high-sensitivity C-reactive protein (Figure S2). We did not observe direct relations between the longitudinal changes in LV indexes and systemic inflammatory markers (Figure S2).

### Change in PWV and History of Diabetes Mellitus

Between visits 1 and 2, PWV increased by 10.9% ( $P<0.0001$ ; Table 2). A greater longitudinal increase in PWV was related to higher age, heart rate, and pulse pressure at baseline ( $P\leq 0.017$ ) and greater increase in heart rate during follow-up ( $P\leq 0.011$ ; Table S6). After adjustment for these important confounders, the longitudinal increase in PWV was more pronounced in participants with a history of diabetes mellitus at baseline as compared

with those without (+1.46 m/s versus +0.71 m/s,  $P=0.039$  [Table S6]). We did not observe any significant association of PWV with insulin or HOMA-IR measured at baseline or follow-up ( $P\geq 0.089$ ).

### Discussion

In this longitudinal, community-based study, we explored the impact of hyperinsulinemia and insulin resistance on temporal changes in LV structure and function as assessed by echocardiography. The key finding of our study was that higher level of serum insulin at baseline and its increase during follow-up independently predicted an increase in LVMI and worsening in LV systolic and diastolic function over time. We also observed high interrelations of temporal changes in LV structure and function indexes. In addition, we showed that participants with a history of diabetes mellitus exhibited greater arterial stiffening over time than participants without diabetes mellitus.

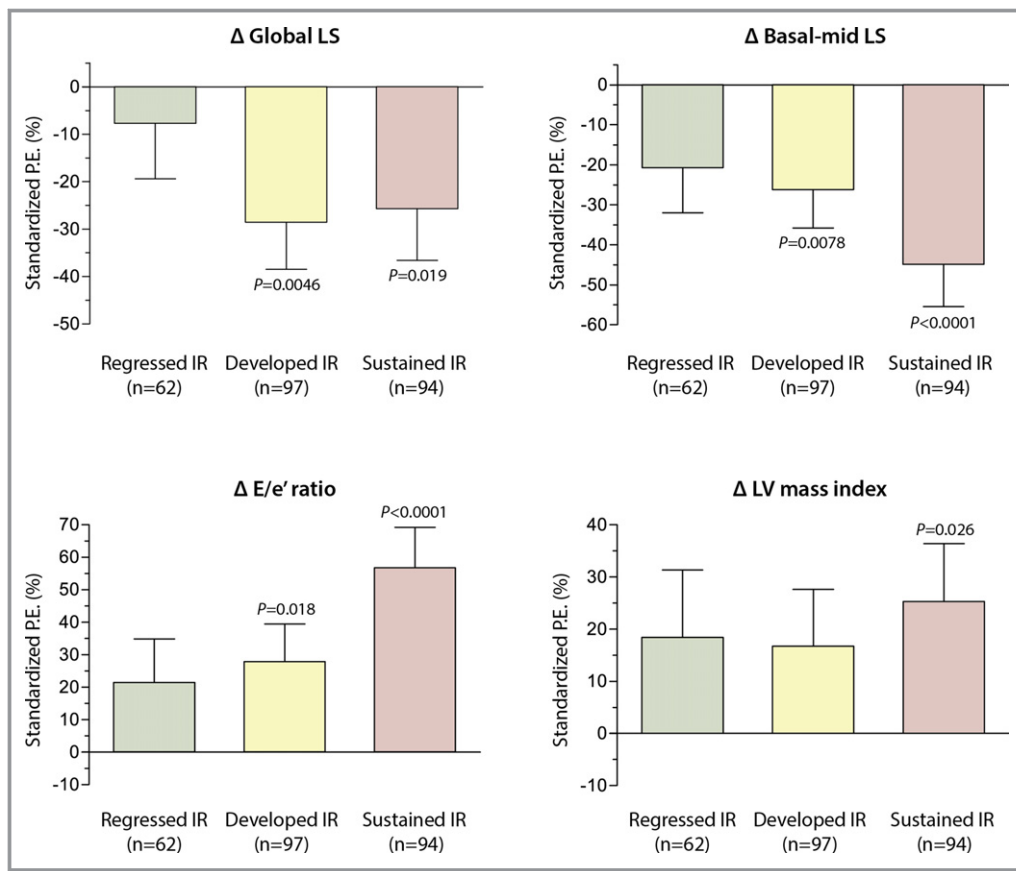


**Figure 2.** Multivariable-adjusted parameter estimates ( $\pm$ SE) for 4.7 years of change ( $\Delta$ ) in left ventricular (LV) longitudinal strain (LS), E/e', and LV mass index in patients with regression, development, or persistence of insulin resistance (IR) during follow-up. Adjusted parameter estimates (PEs) are expressed as percentage of SD of the longitudinal change in LV index. *P* values are for comparisons with the reference group, which includes patients who had normal Homeostatic Model Assessment of Insulin Resistance at baseline and follow-up (*n*=374). Analyses were adjusted for follow-up duration, baseline LV index, age, sex, heart rate, body height, body weight, pulse pressure, and mean arterial pressure. We additionally adjusted for longitudinal changes in these risk factors and for 3 indicator variables coding for antihypertensive drug class intake (starting or stopping treatment between baseline and follow-up and remaining on treatment).

Recent HF guidelines emphasized the need for better understanding and management of risk factors triggering the subclinical LV dysfunction that precedes HF symptoms by years to decades.<sup>4</sup> Indeed, the myocardium already undergoes structural and metabolic changes in the presence of cardiovascular risk factors years to decades before symptomatic HF emerges. Within this context, insulin resistance along with other cardiovascular factors might play an important role in the initiation and progression of cardiac remodeling and dysfunction.

Numerous experimental studies clarified the mechanisms of insulin resistance on LV contractility and stiffness.<sup>5–7</sup> The normal unstressed heart mainly relies on oxidation of FFAs for energy production, but is able to switch to more energy-efficient glycolysis during the stressed state such as pressure load, ischemia, or injury. Insulin resistance leads to a decrease of the glucose uptake by cardiomyocytes and,

therefore, to a lower glycolysis rate.<sup>22,23</sup> The heart responds by augmenting FFA metabolism, which, in turn, leads to increased oxygen consumption, decreased cardiac efficiency, and lipotoxicity.<sup>7</sup> In addition to a disturbance in energy production, compensatory excess of FFA uptake dysregulates the cellular  $\text{Ca}^{2+}$  handling, thereby disturbing the myocardial excitation-contraction coupling.<sup>24</sup> Furthermore, insulin resistance is linked to sympathetic dysregulation, mitochondrial dysfunction, increased oxidative stress, low-grade chronic inflammation, and irreversible deposition of advanced glycation end-products in the coronary microvasculature.<sup>7</sup> Importantly, the cascade of metabolic dysregulations triggered by insulin resistance is responsible for the cardiac dysfunction even before systemic hyperglycemia.<sup>25</sup>

So far, previous population studies have described the relation of LV structure and function with insulin resistance in a cross-sectional manner. For instance, 2 cross-sectional,



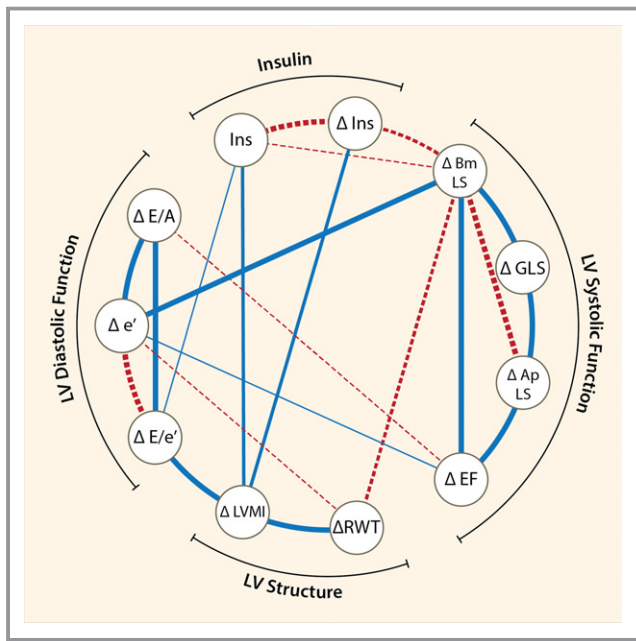


**Figure 3.** Partial correlation diagram between 4.7 years of change ( $\Delta$ ) in left ventricular (LV) structure and function and insulin. The full and dashed lines represent direct and inverse correlations, respectively ( $P < 0.05$  for all). Thicker lines imply stronger relationships. LV changes were adjusted as explained in the footnote to Table 3. ApLS indicates apical longitudinal strain; BmLS, basal-mid longitudinal strain; EF, ejection fraction; GLS, global longitudinal strain measured in the apical 4-chamber view; Ins, insulin; LVMI, LV mass index; RWT, relative wall thickness.

community-based studies demonstrated an independent association between the degree of insulin resistance (by HOMA-IR) and increased LVMI and LV mass to volume ratio assessed by MRI.<sup>10,11</sup> In addition, insulin resistance was also associated with LV diastolic dysfunction, namely with increased

E/e' and decreased TDI e' velocity.<sup>12,13</sup> Another cross-sectional analysis in 6231 Framingham participants showed that worse LS was, independently of other obesity-related phenotypes, associated with higher values of HOMA-IR.<sup>14</sup> In the CARDIA (Coronary Artery Risk Development in Young Adults) study ( $n=3179$ ), participants belonging to the impaired glucose tolerance group had higher relative wall thickness and lower LS and e' peak measured 25 years after initial examination compared with the group with normal glucose metabolism at baseline.<sup>15</sup> However, the authors could not evaluate temporal changes in LV indexes in relation to insulin resistance because echocardiography was performed only at the final follow-up examination.<sup>15</sup> Also, statistical analysis in the CARDIA study was limited to comparisons of LV traits between different groups of glucose metabolism.

Serial imaging studies remain essential to better understand subclinical LV deterioration over time and to assess the role of insulin resistance herein. Longitudinal community-based studies showed that, in parallel with adverse changes in cardiac geometry, LV systolic and diastolic function tends to worsen over the adult life course, particularly in the presence of risk factors such as hypertension and diabetes mellitus.<sup>20,21,26,27</sup> In our longitudinal study, for the first time, we comprehensively assessed in both continuous and categorical analyses the impact of insulin resistance on the natural history of LV remodeling and dysfunction, while considering the complex interrelations between the longitudinal LV changes. We showed that higher levels of insulin at baseline and its increase over follow-up were associated with the decline in LV systolic performance (by LS and EF), worsening of diastolic function (by E/e'), and the increase in LVMI (Figure 4).

Arterial stiffening is another consequence of diabetes mellitus. Several studies in healthy patients and those with

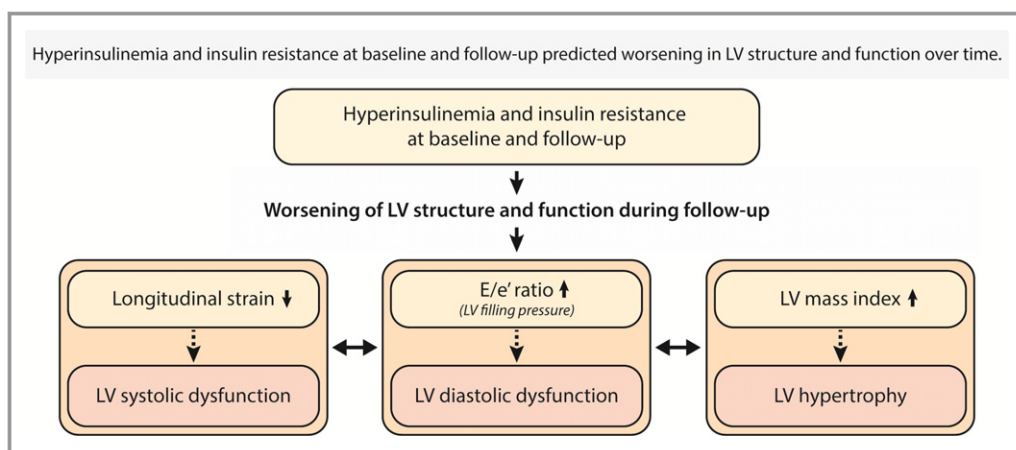


**Figure 4.** Relation of insulin resistance to longitudinal changes in left ventricular (LV) structure and function. In this longitudinal population study, progression of insulin resistance status during follow-up was associated with the decline in LV systolic performance (by longitudinal strain), worsening of diastolic function (by E/e'), and increase in LV mass index.

diabetes mellitus found a link between higher aortic stiffness (by PWV) and diabetes mellitus.<sup>28</sup> For instance, the Malmö Diet and Cancer Study prospectively observed an independent relation between baseline insulin resistance and PWV measured 16 years after the initial examination.<sup>29</sup> Similar to our findings, de Oliveira Alvim et al<sup>30</sup> showed that over 5 years of follow-up, PWV increased by 0.4 m/s in 355 patients without diabetes mellitus and by 1.5 m/s in 25 patients with diabetes mellitus. Thus, the accelerated arterial stiffening found in patients with diabetes mellitus might be a consequence of the activation of proinflammatory factors, the irreversible deposition of advanced glycation end-products in the arterial wall, and increased oxidative stress, leading to vasculopathy.<sup>28,31</sup> Along these lines, we observed that markers of systemic inflammation such as high-sensitivity C-reactive protein and high-sensitivity interleukin 6 increased more over time with higher baseline insulin.

Our findings suggest that insulin resistance mediates the subclinical deterioration of LV performance besides important cardiovascular risk factors. As such, early detection and effective management of insulin resistance may prevent or delay the development of subclinical LV remodeling and dysfunction preceding metabolic cardiomyopathy and symptomatic HF. These strategies might tackle the rising contribution of (pre)diabetes mellitus to the epidemic of symptomatic HF.

## Study Limitations

Our study has to be interpreted within the context of its potential limitations and strengths. First, echocardiographic measurements are prone to measurement errors as a result of signal noise, acoustic artefacts, and angle dependency. In the present study, an experienced observer recorded all echocardiographic images using a standardized imaging protocol at baseline and follow-up. All digitally stored images were centrally postprocessed by 2 experienced observers with good reproducibility. Second, in our study, we did not evaluate LV deformation in circumferential and radial direction. However, LV longitudinal strain appears to be the most robust echocardiographic metric with independent predictive value<sup>16</sup> as compared with circumferential and radial strain, and therefore it might be easily implemented in clinical practice to detect subclinical systolic dysfunction in high-risk patients. Third, our study population included only white Europeans, limiting the extrapolation of our findings to other ethnicities.

## Conclusions

In this longitudinal population study, increased insulin resistance at baseline and during follow-up predicted LV hypertrophy and worsening in LV systolic and diastolic function

over time. Patients with a history of diabetes mellitus exhibited stronger arterial stiffening as compared with participants without diabetes mellitus. Our findings underscore the importance of management of insulin resistance in patients at risk for cardiovascular disease.

## Sources of Funding

The European Union (HEALTH-F7-305507 HOMAGE) and European Research Council (ERC Advanced Grant-2011-294713-EPLORE, PoC Grant 713601-uPROPHET) supported the Studies Coordinating Centre (Leuven, Belgium). The Studies Coordinating Centre also received grants from the Fonds voor Wetenschappelijk Onderzoek Vlaanderen, Brussels, Belgium (grants G.0880.13, G.0881.13 and 11Z0916N).

## Disclosures

None.

## References

1. Dei Cas A, Khan SS, Butler J, Mentz RJ, Bonow RO, Avogaro A, Tschoepe D, Doehner W, Greene SJ, Senni M, Gheorghiade M, Fonarow GC. Impact of diabetes on epidemiology, treatment, and outcomes of patients with heart failure. *JACC Heart Fail*. 2015;3:136–145.
2. Bertoni AG, Hundley WG, Massing MW, Bonds DE, Burke GL, Goff DC. Heart failure prevalence, incidence, and mortality in the elderly with diabetes. *Diabetes Care*. 2004;27:699–703.
3. MacDonald MR, Jhund PS, Petrie MC, Lewsey JD, Hawkins NM, Bhagra S, Munoz N, Varyani F, Redpath A, Chalmers J, MacIntyre K, McMurray JJ. Discordant short- and long-term outcomes associated with diabetes in patients with heart failure: importance of age and sex: a population study of 5.1 million people in Scotland. *Circ Heart Fail*. 2008;1:234–241.
4. Yancy CW, Jessup M, Bozkurt B, Butler J, Casey DE Jr, Drazner MH, Fonarow GC, Geraci SA, Horwich T, Januzzi JL, Johnson MR, Kasper EK, Levy WC, Masoudi FA, McBride PE, McMurray JJ, Mitchell JE, Peterson PN, Riegel B, Sam F, Stevenson LW, Tang WH, Tsai EJ, Wilkoff BL. 2013 ACCF/AHA guideline for the management of heart failure: a report of the American College of Cardiology Foundation/American Heart Association Task Force on Practice Guidelines. *J Am Coll Cardiol*. 2013;62:e147–e239.
5. Ouwens DM, Boer C, Fodor M, de Galan P, Heine RJ, Maassen JA, Diamant M. Cardiac dysfunction induced by high-fat diet is associated with altered myocardial insulin signalling in rats. *Diabetologia*. 2005;48:1229–1237.
6. Velez M, Kohli S, Sabbah HN. Animal models of insulin resistance and heart failure. *Heart Fail Rev*. 2014;19:1–13.
7. Witteles RM, Fowler MB. Insulin-resistant cardiomyopathy clinical evidence, mechanisms, and treatment options. *J Am Coll Cardiol*. 2008;51:93–102.
8. An D, Rodrigues B. Role of changes in cardiac metabolism in development of diabetic cardiomyopathy. *Am J Physiol Heart Circ Physiol*. 2006;291:H1489–H1506.
9. Nishida K, Otsu K. Inflammation and metabolic cardiomyopathy. *Cardiovasc Res*. 2017;113:389–398.
10. Velagaleti RS, Gona P, Chuang ML, Salton CJ, Fox CS, Blease SJ, Yeon SB, Manning WJ, O'Donnell CJ. Relations of insulin resistance and glycemic abnormalities to cardiovascular magnetic resonance measures of cardiac structure and function: the Framingham Heart Study. *Circ Cardiovasc Imaging*. 2010;3:257–263.
11. Shah RV, Abbasi SA, Heydari B, Rickers C, Jacobs DR Jr, Wang L, Kwong RY, Bluemke DA, Lima JA, Jerosch-Herold M. Insulin resistance, subclinical left ventricular remodeling, and the obesity paradox: MESA (Multi-Ethnic Study of Atherosclerosis). *J Am Coll Cardiol*. 2013;61:1698–1706.
12. Demmer RT, Allison MA, Cai J, Kaplan RC, Desai AA, Hurwitz BE, Newman JC, Shah SJ, Swett K, Talavera GA, Thai A, Youngblood ME, Rodriguez CJ. Association of impaired glucose regulation and insulin resistance with cardiac

- structure and function: results from ECHO-SOL (Echocardiographic Study of Latinos). *Circ Cardiovasc Imaging*. 2016;9:e005032.
13. Fontes-Carvalho R, Ladeiras-Lopes R, Bettencourt P, Leite-Moreira A, Azevedo A. Diastolic dysfunction in the diabetic continuum: association with insulin resistance, metabolic syndrome and type 2 diabetes. *Cardiovasc Diabetol*. 2015;14:4.
  14. Ho JE, McCabe EL, Wang TJ, Larson MG, Levy D, Tsao C, Aragam J, Mitchell GF, Benjamin EJ, Vasan RS, Cheng S. Cardiometabolic traits and systolic mechanics in the community. *Circ Heart Fail*. 2017;10:e003536.
  15. Kishi S, Gidding SS, Reis JP, Colangelo LA, Venkatesh BA, Armstrong AC, Isogawa A, Lewis CE, Wu C, Jacobs DR Jr, Liu K, Lima JA. Association of insulin resistance and glycemic metabolic abnormalities with LV structure and function in middle age: the CARDIA study. *JACC Cardiovasc Imaging*. 2017;10:105–114.
  16. Kuznetsova T, Cauwenberghs N, Knez J, Yang WY, Herbots L, D'hooge J, Haddad F, Thijs L, Voigt JU, Staessen JA. Additive prognostic value of left ventricular systolic dysfunction in a population-based cohort. *Circ Cardiovasc Imaging*. 2016;9:e004661.
  17. Lang RM, Badano LP, Mor-Avi V, Afkalo J, Armstrong A, Ernande L, Flachskampf FA, Foster E, Goldstein SA, Kuznetsova T, Lancellotti P, Muraru D, Picard MH, Rietzschel ER, Rudski L, Spencer KT, Tsang W, Voigt JU. Recommendations for cardiac chamber quantification by echocardiography in adults: an update from the American Society of Echocardiography and the European Association of Cardiovascular Imaging. *J Am Soc Echocardiogr*. 2015;28:1–39.e14.
  18. Laurent S, Cockcroft J, Van Bortel L, Boutouyrie P, Giannattasio C, Hayoz D, Pannier B, Vlachopoulos C, Wilkinson I, Struijker-Boudier H. Expert consensus document on arterial stiffness: methodological issues and clinical applications. *Eur Heart J*. 2006;27:2588–2605.
  19. Balkau B, Charles MA. Comment on the provisional report from the WHO consultation. European Group for the Study of Insulin Resistance (EGIR). *Diabet Med*. 1999;16:442–443.
  20. Cauwenberghs N, Knez J, D'hooge J, Thijs L, Yang WY, Wei FF, Zhang ZY, Staessen JA, Kuznetsova T. Longitudinal changes in LV structure and diastolic function in relation to arterial properties in general population. *JACC Cardiovasc Imaging*. 2017;10:1307–1316.
  21. Kuznetsova T, Thijs L, Knez J, Cauwenberghs N, Petit T, Gu YM, Zhang Z, Staessen JA. Longitudinal changes in left ventricular diastolic function in a general population. *Circ Cardiovasc Imaging*. 2015;8:e002882.
  22. Szablewski L. Glucose transporters in healthy heart and in cardiac disease. *Int J Cardiol*. 2017;230:70–75.
  23. Gibbs EM, Stock JL, McCoid SC, Stukenbrok HA, Pessin JE, Stevenson RW, Milici AJ, McNeish JD. Glycemic improvement in diabetic db/db mice by overexpression of the human insulin-regulatable glucose transporter (GLUT4). *J Clin Invest*. 1995;95:1512–1518.
  24. Lebeche D, Davidoff AJ, Hajjar RJ. Interplay between impaired calcium regulation and insulin signaling abnormalities in diabetic cardiomyopathy. *Nat Clin Pract Cardiovasc Med*. 2008;5:715–724.
  25. Buchanan J, Mazumder PK, Hu P, Chakrabarti G, Roberts MW, Yun UJ, Cooksey RC, Litwin SE, Abel ED. Reduced cardiac efficiency and altered substrate metabolism precedes the onset of hyperglycemia and contractile dysfunction in two mouse models of insulin resistance and obesity. *Endocrinology*. 2005;146:5341–5349.
  26. Lieb W, Xanthakis V, Sullivan LM, Aragam J, Pencina MJ, Larson MG, Benjamin EJ, Vasan RS. Longitudinal tracking of left ventricular mass over the adult life course: clinical correlates of short- and long-term change in the Framingham Offspring Study. *Circulation*. 2009;119:3085–3092.
  27. Lieb W, Xanthakis V, Sullivan LM, Aragam J, Pencina MJ, Larson MG, Benjamin EJ, Vasan RS. The natural history of left ventricular geometry in the community: clinical correlates and prognostic significance of change in LV geometric pattern. *JACC Cardiovasc Imaging*. 2014;7:870–878.
  28. Prenalier SB, Chirinos JA. Arterial stiffness in diabetes mellitus. *Atherosclerosis*. 2015;238:370–379.
  29. Gottsater M, Ostling G, Persson M, Engstrom G, Melander O, Nilsson PM. Non-hemodynamic predictors of arterial stiffness after 17 years of follow-up: the Malmö Diet and Cancer study. *J Hypertens*. 2015;33:957–965.
  30. de Oliveira Alvim R, Santos PC, Musso MM, de Sá Cunha R, Krieger JE, Mill JG, Pereira AC. Impact of diabetes mellitus on arterial stiffness in a representative sample of an urban Brazilian population. *Diabetol Metab Syndr*. 2013;5:45.
  31. Mazzone T, Chait A, Plutzky J. Cardiovascular disease risk in type 2 diabetes mellitus: insights from mechanistic studies. *Lancet*. 2008;371:1800–1809.

# **SUPPLEMENTAL MATERIAL**

## Data S1.

## Supplemental Methods

### ECHOCARDIOGRAPHY

The participants refrained from smoking, heavy exercise and drinking alcohol or caffeine-containing beverages for at least 3 hours prior to the examination. To ensure steady state, echocardiography and arterial measurements were obtained consecutively and after the subjects had rested for at least 15 min in the supine position.

**Data acquisition.** One experienced physician (T.K.) did both echocardiographic examinations using a Vivid7 Pro and Vivid E9 (GE Vingmed, Horten, Norway), respectively, interfaced with a 2.5- to 3.5-MHz phased-array probe. The observer obtained M-mode recordings of the LV from the parasternal long axis view guided by the 2D image. The ultrasound beam was positioned just below the mitral valve at the level of the posterior chordae tendineae. Gray-scale images were obtained from the parasternal long and short axes and from the apical 4- and 2-chamber and long-axis views. From the apical window, the observer positioned a 1- to 3-mm Doppler sample volume at the mitral valve tips to record pulsed wave Doppler transmitral flow velocities. The sonographer placed a 5-mm tissue Doppler sample at septal, lateral, inferior and posterior sites of the mitral annulus to record mitral annular velocity patterns. All digitally stored recordings included at least 5 cardiac cycles.

**Off-line analysis.** One observer (T.K.) analyzed the echocardiograms blinded to the participants' characteristics using EchoPac software, version BT13 (GE Vingmed, Horten, Norway). All measurements were averaged over three heart cycles for statistical analysis. LV internal diameter and interventricular septal and posterior wall thickness were measured from the 2D-guided M-mode tracing at end-diastole. Relative wall thickness (RWT) was calculated as  $0.5 \times (\text{interventricular septum} + \text{posterior wall}) / \text{LV internal diameter at end-diastole}$ . LV



dimensions were used to calculate LV mass via an anatomically validated formula. Left atrial (LA) volume was calculated by the prolate-ellipsoid method from LA dimensions measured in the parasternal long, lateral and supero-inferior axes. LA volume and LV mass was indexed to body surface area (BSA), calculated as  $\text{body weight}^{0.425} \text{ (in kg)} \times \text{body height}^{0.725} \text{ (in cm)} \times 0.007184$ . Using the standard Simpson method, LV end-diastolic volume (EDV), end-systolic volume (ESV) and ejection fraction (EF) were derived from the apical 4- and 2 chamber views. Transmitral blood flow signals were used to measure peak early (E) and late (A) diastolic velocity. From the Tissue Doppler Imaging (TDI) recordings, we measured the peak systolic (s') and early diastolic (e') velocities of the mitral annulus at septal, lateral, inferior and posterior acquisition sites. E/e' ratio was calculated by dividing transmitral E peak by e' averaged from the 4 acquisition sites.

**2D LV strain.** Two observers (T.K. and N.C.) derived LV longitudinal strain (LS) using a myocardial speckle-tracking software package (Q-analysis, GE Vingmed) at default settings. The LV endocardial border was manually traced at the end-systolic frame of the 2D apical 4-chamber view. The software automatically tracked myocardial speckle motion while dividing the region of interest in LV basal, mid and apical levels. We adjusted the region of interest to the myocardial thickness and further adjustments were made after visual evaluation of the tracking. Images were rejected when tracking was inadequate in  $\geq 2$  segments. We obtained basal-mid and apical LS by averaging the segmental LS of the respective regions. We used absolute values of peak systolic midwall LS for statistical analysis.

## Reproducibility

The data on intra-observer reproducibility was published elsewhere [see ref 16]. To further assess the inter-observer reproducibility for assessment of LS, two experienced observers (T.K. and N.C.) measured in duplicates LV 4-chamber LS in 53 subjects. The reproducibility was estimated, using the Bland-Altman plots. The absolute bias was calculated as the difference between the observers' measurements ( $x_2 - x_1$ ) and was plotted against their average ( $(x_2 + x_1) / 2 = \text{average } x$ ). The relative bias was calculated as the difference between paired readings, divided by the average ( $((x_1 - x_2) / \text{average } x) \times 100$ ) and was plotted against the average value of repeated

readings (average  $\bar{x}$ ). For the inter-observer (T.K. and N.C.) variability, the mean absolute and relative differences between pairwise readings for 4-chamber LS were  $0.040 \pm 1.38\%$  and  $0.25 \pm 7.23\%$  respectively.

**Table S1. Clinical Characteristics of Men and Women at Baseline and Follow-up Examination.**

Characteristic	Men (n = 305)			Women (n = 322)		
	Visit 1 (2005-2009)	Visit 2 (2009-2013)	P value	Visit 1 (2005-2009)	Visit 2 (2009-2013)	P value
<i>Anthropometrics</i>						
Age, y	50.3 ± 14.7	55.0 ± 14.6	<0.0001	50.8 ± 14.5	55.5 ± 14.4	<0.0001
Body mass index, kg/m <sup>2</sup>	26.6 ± 3.45	27.4 ± 3.59	<0.0001	26.2 ± 4.70	26.8 ± 4.67	<0.0001
Waist circumference, cm	94.2 ± 9.78	98.7 ± 10.3	<0.0001	85.9 ± 12.5	92.1 ± 13.1	<0.0001
Brachial systolic BP, mm Hg	130.0 ± 14.5	132.6 ± 15.0	0.0002	127.2 ± 18.5	131.6 ± 18.4	<0.0001
Brachial diastolic BP, mm Hg	81.9 ± 9.27	83.7 ± 9.55	0.0003	77.8 ± 9.06	80.8 ± 9.70	<0.0001
Brachial pulse pressure, mm Hg	48.1 ± 12.4	48.9 ± 14.2	0.18	49.4 ± 15.6	50.7 ± 16.7	0.050
Mean arterial pressure, mm Hg	97.9 ± 9.6	100.0 ± 9.5	<0.0001	94.2 ± 10.7	97.7 ± 10.7	<0.0001
Heart rate, bpm	58.4 ± 9.09	58.1 ± 9.17	0.48	62.2 ± 9.24	61.8 ± 9.72	0.42
<i>Questionnaire data</i>						
Current smoking, n (%)	64 (21.0)	50 (16.4)	0.0005	57 (17.7)	48 (14.9)	0.012
Drinking alcohol, n (%)	185 (60.7)	168 (55.1)	0.046	74 (23.0)	71 (22.0)	0.77
Hypertensive, n (%)	138 (45.2)	166 (54.4)	0.0005	121 (37.6)	150 (46.6)	<0.0001
Treated for hypertension, n (%)	73 (23.9)	103 (33.8)	<0.0001	81 (25.2)	100 (31.1)	0.0003
β-blockers, n (%)	46 (15.1)	55 (18.0)	0.093	48 (14.9)	52 (16.1)	0.50
ACE or ARB, n (%)	26 (8.52)	41 (13.4)	0.0059	25 (7.76)	45 (14.0)	<0.0001
CCB or α-blockers, n (%)	14 (4.59)	35 (11.5)	0.0002	12 (3.73)	20 (6.21)	0.039
Diuretics, n (%)	19 (6.23)	31 (10.2)	0.017	36 (11.2)	38 (11.8)	0.84
History of CHD, n (%)	16 (5.25)	35 (11.5)	<0.0001	6 (1.86)	9 (2.80)	0.25
History of diabetes, n (%)	10 (3.28)	23 (7.54)	0.0002	11 (3.42)	25 (7.76)	0.0001
<i>Biochemical data</i>						
Serum creatinine, μmol/L	93.9 ± 15.3	98.3 ± 25.7	<0.0001	78.6 ± 11.6	81.3 ± 15.8	<0.0001
Total cholesterol, mmol/L	5.13 ± 0.94	4.83 ± 0.89	<0.0001	5.41 ± 0.95	5.20 ± 0.97	<0.0001
hs-CRP, mg/L	1.23 (0.51-2.85)	1.37 (0.69 -3.65)	0.24	1.81 (0.76-7.42)	1.62 (0.74 -5.60)	0.059
hs-IL6, pg/mL	1.37 (0.68-3.04)	1.48 (0.69 -3.54)	0.21	1.55 (0.59-3.59)	1.49 (0.62-3.43)	0.48
Blood glucose, mmol/L	5.02 ± 0.85	4.99 ± 0.68	0.57	4.81 ± 0.59	4.84 ± 0.75	0.65
Serum insulin, μmol/L	4.66 (2.00-9.00)	5.15 (2.30-12.0)	0.0054	4.79 (2.00-11.0)	5.12 (2.00-12.0)	0.074
HOMA-IR	1.07 (0.13-6.77)	1.35 (0.19-10.4)	0.016	1.04 (0.14-9.07)	1.22 (0.15-7.70)	0.096

Values are mean (±SD), number of subjects (%) or geometric mean (10-90% percentile interval). ACE indicates angiotensin-converting enzyme; ARB, angiotensin receptor blockers; BP, blood pressure; bpm, beats per minute; CCB, calcium channel blockers and CHD, coronary heart disease; HOMA-IR, Homeostatic Model Assessment of Insulin Resistance; hs-CRP, high-sensitivity C-reactive protein; hs-IL6, high-sensitivity interleukin-6.

**Table S2. PWV and Echocardiographic Characteristics of Men and Women at Baseline and Follow-up Examination.**

Characteristic	Men (n = 305)			Women (n = 322)		
	Visit 1 (2005-2009)	Visit 2 (2009-2013)	P value	Visit 1 (2005-2009)	Visit 2 (2009-2013)	P value
Pulse wave velocity, m/s	7.59 ± 1.71	8.33 ± 2.07*	<0.0001	7.30 ± 1.75	7.94 ± 2.09*	<0.0001
<i>LV structure</i>						
Internal diameter, cm	5.26 ± 0.42	5.23 ± 0.40	0.082	4.85 ± 0.37	4.83 ± 0.35	0.18
Septal wall, cm	1.04 ± 0.15	1.07 ± 0.14	0.0001	0.91 ± 0.14	0.94 ± 0.14	<0.0001
Posterior wall, cm	0.95 ± 0.13	1.00 ± 0.11	<0.0001	0.84 ± 0.13	0.89 ± 0.11	<0.0001
Relative wall thickness, cm	0.38 ± 0.06	0.40 ± 0.06	<0.0001	0.36 ± 0.06	0.38 ± 0.05	<0.0001
Mass index, g/m <sup>2</sup>	100.3 ± 20.0	103.4 ± 20.2	<0.0001	84.1 ± 18.5	88.3 ± 19.4	<0.0001
Length, cm	8.58 ± 0.66	8.51 ± 0.63	0.051	7.69 ± 0.56	7.72 ± 0.58	0.21
EDV, ml	115.5 ± 22.7	110.0 ± 22.6	0.0002	84.4 ± 17.6	79.9 ± 17.2	<0.0001
ESV, ml	43.9 ± 11.0	43.7 ± 10.8	0.79	30.9 ± 8.27	30.3 ± 7.75	0.019
<i>LV systolic function</i>						
Ejection fraction, %	62.8 ± 6.39	60.2 ± 6.22	<0.0001	64.2 ± 6.40	62.1 ± 6.49	<0.0001
TDI s' peak, cm/s <sup>#</sup>	9.51 ± 1.35	8.29 ± 1.25	<0.0001	8.67 ± 1.34	7.77 ± 1.29	<0.0001
Global LS, %	18.9 ± 2.22	18.7 ± 2.16	0.032	20.4 ± 2.27	20.3 ± 2.27	0.38
Basal-mid LS, %	17.9 ± 2.15	17.8 ± 2.04	0.83	19.1 ± 2.20	19.3 ± 2.06	0.071
Apical LS, %	22.6 ± 4.21	21.2 ± 3.39	<0.0001	24.3 ± 4.08	22.9 ± 3.96	<0.0001
<i>LV diastolic function</i>						
LA volume index, ml/m <sup>2</sup>	24.0 ± 5.94	27.0 ± 6.29	<0.0001	22.0 ± 6.03	24.7 ± 6.78	<0.0001
E peak, cm/s	71.8 ± 15.3	62.9 ± 14.4	<0.0001	79.8 ± 15.7	71.1 ± 15.9	<0.0001
A peak, cm/s	61.0 ± 16.2	57.5 ± 14.2	<0.0001	68.0 ± 16.9	64.2 ± 15.3	<0.0001
E/A ratio	1.28 ± 0.50	1.17 ± 0.44	<0.0001	1.25 ± 0.43	1.19 ± 0.47	<0.0001
TDI e' peak, cm/s <sup>#</sup>	11.5 ± 3.56	9.66 ± 3.25	<0.0001	11.5 ± 3.44	9.96 ± 3.46	<0.0001
TDI a' peak, cm/s <sup>#</sup>	10.5 ± 2.09	9.80 ± 2.11	<0.0001	9.89 ± 1.99	9.34 ± 2.09	<0.0001
E/e' ratio <sup>#</sup>	6.63 ± 1.88	6.96 ± 2.00	<0.0001	7.43 ± 2.27	7.80 ± 2.75	<0.0001

Values are mean (±SD). \*Follow-up measurements of pulse wave velocity were available in 420 subjects. <sup>#</sup>Average of septal, lateral, inferior and posterior mitral annulus sites. 2D indicates two-dimensional; EDV, end-diastolic volume; ESV, end-systolic volume; LA, left atrium; LS, longitudinal strain; LV, left ventricle; TDI, tissue Doppler imaging.

**Table S3. Multivariable-adjusted Associations of 4.7 Years Change in LV Structure and Function with Serum Insulin in 606 Subjects Free of Diabetes Mellitus at Baseline.**

Parameter estimates (95% CI) are the changes in the LV indices associated with a doubling of the baseline

	Baseline serum insulin, per doubling		$\Delta$ Serum insulin, per doubling of the percentage increase	
	Parameter estimate (95% CI)	P value	Parameter estimate (95% CI)	P value
<i>LV structure</i>				
$\Delta$ Internal diameter, cm	-5.70% (-16.3, 4.92)	0.30	-4.86% (-14.7, 4.97)	0.33
$\Delta$ Septal wall, cm	3.66% (-6.83, 14.1)	0.49	7.01% (-2.72, 16.7)	0.16
$\Delta$ Posterior wall, cm	10.4% (1.18, 19.6)	0.027	4.21% (-1.18, 12.7)	0.33
$\Delta$ Relative wall thickness	8.87% (-1.58, 19.3)	0.096	7.27% (-2.41, 17.0)	0.14
$\Delta$ Mass index, g/m <sup>2</sup>	12.7% (2.85, 22.5)	0.012	8.58% (-1.48, 18.6)	0.094
$\Delta$ EDV, ml	-8.43% (-20.0, 3.13)	0.15	-11.2% (-21.9, -0.54)	0.040
$\Delta$ ESV, ml	2.73% (-8.69, 14.1)	0.64	6.47% (-4.12, 17.1)	0.23
<i>LV systolic function</i>				
$\Delta$ Ejection fraction, %	-9.00% (-18.5, 0.52)	0.064	-13.2% (-21.9, -4.50)	0.0030
$\Delta$ Global LS, %	-13.4% (-23.7, -3.03)	0.011	-14.7% (-24.2, -5.15)	0.0026
$\Delta$ Basal-mid LS, %	-15.9% (-25.8, -5.87)	0.0019	-15.3% (-24.5, -6.24)	0.0010
$\Delta$ Apical LS, %	-3.48% (-12.9, 5.91)	0.47	-5.27% (-13.7, 3.11)	0.22
<i>LV diastolic function</i>				
$\Delta$ E peak, cm/s	7.63% (-2.68, 17.9)	0.15	-3.59% (-13.1, 5.87)	0.46
$\Delta$ E/A	2.53% (-7.75, 12.8)	0.63	-9.29% (-18.8, 0.21)	0.055
$\Delta$ TDI e' peak, cm/s	-12.0% (-23.1, -0.90)	0.034	-14.3% (-24.5, -4.14)	0.0059
$\Delta$ E/e'	25.2% (13.1, 37.3)	<0.0001	11.0 (-0.21, 22.1)	0.055

insulin (second column) or a doubling of the longitudinal percentage increase in insulin (fourth column). The parameter estimates are expressed as a percentage of SD of the longitudinal change in LV index. Analyses were adjusted for follow-up duration, baseline LV index, age, sex, heart rate, body height, body weight, pulse pressure and mean arterial pressure. We additionally adjusted for longitudinal changes in these risk factors and for 3 indicator variables coding for antihypertensive drug class intake (starting or stopping treatment between baseline and follow-up and remaining on treatment). All covariables were identified based on stepwise regression analyses. For LV mass index, models did not include anthropometric characteristics. EDV indicates end-diastolic volume; ESV, end-systolic volume; LS, longitudinal strain; LV, left ventricular; TDI, Tissue Doppler Imaging.



**Table S4. Multivariable-adjusted Associations of 4.7 Years Change in LV Structure and Function with Blood Glucose and HOMA-IR.**

	Blood glucose				HOMA-IR			
	Baseline, +0.73 mmol/L		$\Delta$ , +0.83 mmol/L		Baseline, per doubling		$\Delta$ , per doubling of the percentage increase	
	Parameter estimate (95% CI)	P value	Parameter estimate (95% CI)	P value	Parameter estimate (95% CI)	P value	Parameter estimate (95% CI)	P value
<i>LV structure</i>								
$\Delta$ Internal diameter, cm	-1.40% (-10.4, 7.62)	0.76	-1.99% (-10.8, 6.82)	0.65	0.15% (-3.58, 4.24)	0.94	0.10% (-3.58, 3.77)	0.96
$\Delta$ Septal wall, cm	5.53% (-3.16, 14.2)	0.21	2.83% (-5.69, 11.4)	0.51	1.13% (-2.83, 5.09)	0.57	2.34% (-1.22, 5.89)	0.20
$\Delta$ Posterior wall, cm	9.97% (2.29, 17.7)	0.011	1.96% (-5.58, 9.49)	0.61	5.15% (1.66, 8.65)	0.0039	1.74% (-1.41, 4.88)	0.28
$\Delta$ RWT	6.38% (-2.35, 15.1)	0.15	3.63% (-4.93, 12.2)	0.41	2.64% (-1.32, 6.60)	0.19	2.12% (-1.43, 5.68)	0.24
$\Delta$ Mass index, g/m <sup>2</sup>	6.46% (-3.38, 16.3)	0.20	1.69% (-7.91, 11.3)	0.73	6.53% (2.71, 10.4)	0.0009	4.50% (0.78, 8.23)	0.018
$\Delta$ EDV, ml	4.37% (-4.66, 13.4)	0.34	-1.35% (-7.50, 10.2)	0.77	-1.07% (-5.41, 3.27)	0.63	-2.05% (-5.93, 1.82)	0.30
$\Delta$ ESV, ml	3.54% (-5.36, 12.4)	0.43	6.49% (-2.20, 15.2)	0.14	2.67% (-1.54, 6.90)	0.21	3.90% (0.085, 7.71)	0.045
<i>LV systolic function</i>								
$\Delta$ Ejection fraction, %	-3.68% (-11.6, 4.25)	0.36	-5.42% (-13.2, -2.35)	0.17	-4.09% (-7.71, -0.48)	0.027	-5.03% (-8.24, -1.82)	0.0022
$\Delta$ Global LS, %	-7.30% (-16.0, 1.44)	0.10	-7.80% (-16.4, 0.77)	0.074	-6.12% (-10.1, -2.15)	0.0026	-5.72% (-9.26, 2.18)	0.0016
$\Delta$ Basal-mid LS, %	-6.52% (-15.1, 2.03)	0.13	-4.56% (-13.0, 3.84)	0.29	-7.24% (-11.1, -3.35)	0.0003	-6.21% (-9.66, -2.74)	0.0005
$\Delta$ Apical LS, %	-4.62% (-12.7, 3.51)	0.27	-7.09% (-15.1, 0.89)	0.081	-2.27% (-5.92, 1.38)	0.22	-2.46% (-5.62, 0.71)	0.13
<i>LV diastolic function</i>								
$\Delta$ E peak, cm/s	0.31% (-8.68, 9.29)	0.95	1.14% (-7.63, 9.90)	0.80	3.09% (-0.98, 7.15)	0.14	-0.69% (-4.33, 2.95)	0.71
$\Delta$ E/A	-2.83% (-11.5, 5.81)	0.52	0.92% (-7.56, 9.38)	0.83	0.72 % (-3.20, 4.65)	0.71	-2.47% (-5.98, 1.05)	0.17
$\Delta$ TDI e' peak, cm/s	-7.03% (-16.2, 2.18)	0.13	-1.43% (-10.4, 7.59)	0.76	-4.52% (-8.77, -0.28)	0.037	-3.78% (-7.56, -0.02)	0.049
$\Delta$ E/e'	2.24% (-8.01, 12.5)	0.67	2.34% (-7.66, 12.4)	0.65	8.85% (-4.19, 13.5)	0.0002	3.25% (-0.92, 7.43)	0.13

Parameter estimates (95% CI) are the changes in the LV indices associated with a 1-SD in baseline glucose or its change over time and with doubling of the baseline HOMA-IR or a doubling of the longitudinal percentage increase in HOMA-IR. Parameter estimates (95% CI) are expressed as percentage of SD of the longitudinal change in LV index. Analyses were adjusted for follow-up duration, baseline LV index, age, sex, heart rate, body height, body weight, pulse pressure and mean arterial pressure. We additionally adjusted for longitudinal changes in these risk factors and in antihypertensive treatment. Blood glucose was additionally adjusted for insulin levels. All covariables were identified based on stepwise regression analyses. For LV mass index, models did not include anthropometric characteristics. EDV indicates end-diastolic volume; ESV, end-systolic volume; HOMA-IR, homeostatic model assessment of insulin resistance; LS, longitudinal strain; LV, left ventricular; TDI, Tissue Doppler Imaging; RWT, relative wall thickness.

**Figure S5. Clinical and Echocardiographic Characteristics of Participants by Insulin Resistance Group at Baseline and Follow-up Examination.**

Characteristic	Normal HOMA-IR (n=374; 59.7%)	Regressed IR (n=62; 9.89%)	Developed IR (n=97; 15.5%)	Sustained IR (n=94; 14.9%)	P for trend
<i>Clinical characteristics</i>					
Female (%)	193 (51.6%)	36 (58.1%)	50 (51.5%)	43 (45.7%)	0.51
Age, y					
Baseline	49.7 ± 14.1	44.6 ± 15.6	53.5 ± 15.8	54.9 ± 12.7	<0.0001
Follow-up	54.5 ± 14.0	49.3 ± 15.7	58.0 ± 15.8	59.4 ± 12.7	<0.0001
Δ	+4.81 ± 0.51	+4.73 ± 0.72	+4.56 ± 0.63	+4.55 ± 0.59	<0.0001
Body weight, kg					
Baseline	71.8 ± 13.0	78.1 ± 13.4	78.3 ± 11.1	86.7 ± 16.4	<0.0001
Follow-up	73.6 ± 13.3	78.8 ± 13.2	82.7 ± 13.0	88.0 ± 15.5	<0.0001
Δ	+1.84 ± 4.48	+0.65 ± 6.21	+4.32 ± 5.16	+1.25 ± 7.57	<0.0001
PP, mm Hg					
Baseline	47.6 ± 13.7	48.4 ± 13.3	51.8 ± 15.8	50.8 ± 14.3	0.028
Follow-up	48.8 ± 15.2	46.3 ± 13.8	52.4 ± 14.9	54.0 ± 17.7	0.0025
Δ	+1.21 ± 11.4	-2.15 ± 10.2	+0.60 ± 11.3	+3.16 ± 10.9	0.036
MAP, mm Hg					
Baseline	94.8 ± 9.75	94.9 ± 11.4	96.9 ± 9.99	100.9 ± 11.0	<0.0001
Follow-up	97.8 ± 10.0	97.3 ± 8.94	101.2 ± 10.3	101.7 ± 100.5	0.0002
Δ	+2.98 ± 9.09	+2.40 ± 8.66	+4.33 ± 8.89	+0.78 ± 9.27	0.058
Heart rate, bpm					
Baseline	59.0 ± 8.92	63.7 ± 9.70	60.3 ± 8.58	63.3 ± 10.4	<0.0001
Follow-up	58.5 ± 8.92	61.9 ± 9.15	62.1 ± 9.96	62.5 ± 11.2	<0.0001
Δ	-0.46 ± 7.24	-1.86 ± 7.65	+1.76 ± 7.43	-0.87 ± 8.00	0.012
<i>LV structure</i>					
RWT					
Baseline	0.37 ± 0.059	0.36 ± 0.056	0.37 ± 0.059	0.40 ± 0.066	0.0007
Follow-up	0.38 ± 0.052	0.38 ± 0.052	0.40 ± 0.062	0.41 ± 0.049	<0.0001
Δ	0.015 ± 0.051	+0.024 ± 0.042	+0.026 ± 0.056	+0.016 ± 0.058	0.30
Mass index, g/m <sup>2</sup>					
Baseline	90.4 ± 19.3	90.3 ± 23.0	93.5 ± 24.9	97.6 ± 20.0	0.0055
Follow-up	93.2 ± 19.4	94.6 ± 23.2	98.0 ± 24.5	103.3 ± 21.2	<0.0001
Δ	2.78 ± 11.6	+4.31 ± 14.1	+5.11 ± 14.3	+5.65 ± 15.0	0.016
<i>LV systolic function</i>					
EF, %					
Baseline	63.3 ± 6.29	63.0 ± 5.80	63.8 ± 6.28	64.4 ± 7.43	0.85
Follow-up	61.6 ± 6.34	61.2 ± 5.55	60.4 ± 6.25	60.5 ± 7.38	0.035
Δ	-1.74 ± 8.03	+1.83 ± 6.88	-3.30 ± 7.99	-3.96 ± 9.62	0.14
Global LS, %					
Baseline	19.9 ± 2.21	19.7 ± 2.67	19.6 ± 2.49	18.9 ± 2.47	0.0014
Follow-up	19.8 ± 2.26	19.5 ± 2.36	19.0 ± 2.45	18.9 ± 2.48	0.0003
Δ	-0.12 ± 2.28	-0.12 ± 2.38	-0.67 ± 2.22	-0.047 ± 2.49	0.17
Basal-mid LS, %					
Baseline	18.8 ± 2.08	18.4 ± 2.58	18.5 ± 2.53	17.5 ± 2.18	<0.0001
Follow-up	19.0 ± 2.00	18.6 ± 2.30	18.2 ± 2.21	17.5 ± 2.35	<0.0001
Δ	+0.22 ± 2.10	+0.16 ± 2.04	-0.31 ± 2.33	+0.014 ± 2.23	0.0001
Apical LS, %					
Baseline	23.8 ± 4.27	23.4 ± 4.55	23.1 ± 4.00	23.0 ± 4.06	0.27
Follow-up	22.2 ± 3.79	21.9 ± 3.87	21.4 ± 3.58	22.2 ± 3.97	0.25
Δ	-1.55 ± 4.32	-1.47 ± 4.95	-1.64 ± 4.22	-0.78 ± 4.24	0.39
<i>LV diastolic function</i>					
E peak, cm/s					
Baseline	77.8 ± 15.7	76.0 ± 15.9	72.3 ± 16.6	72.0 ± 15.8	0.0037
Follow-up	68.0 ± 14.8	70.5 ± 15.5	63.1 ± 17.2	65.2 ± 17.0	0.016
Δ	-9.84 ± 11.5	-5.49 ± 9.90	-9.27 ± 10.3	-6.73 ± 13.4	0.042

e' peak, cm/s					
Baseline	12.2 ± 3.44	12.2 ± 3.83	10.3 ± 3.63	9.36 ± 2.43	<0.0001
Follow-up	10.4 ± 3.15	10.9 ± 3.63	8.45 ± 3.44	7.95 ± 2.77	<0.0001
Δ	-1.80 ± 1.54	-1.33 ± 1.54	-1.76 ± 1.64	-1.40 ± 1.56	0.032
E/e' ratio					
Baseline	6.72 ± 1.95	6.62 ± 1.80	7.57 ± 2.38	8.03 ± 2.28	<0.0001
Follow-up	6.91 ± 1.98	6.96 ± 1.97	8.14 ± 3.07	8.79 ± 2.98	<0.0001
Δ	+0.19 ± 1.21	+0.34 ± 1.26	+0.57 ± 1.67	+0.76 ± 1.91	0.0002

Values are mean (±SD) or number of subjects (%). EF indicates ejection fraction; HOMA-IR, homeostatic model assessment of insulin resistance; IR, insulin resistance; LS, longitudinal strain; MAP, mean arterial pressure; PP, pulse pressure; LV, left ventricle; RWT, relative wall thickness.

**Table S6. Correlates of 4.7 Years Change in Pulse Wave Velocity in a Subset of 420 Participants.**

	$\Delta$ Pulse wave velocity (m/s)*		
	$\beta \pm \text{SE}$	$R^2$ (%)	$P$ value
$\Delta$ , mean (5-95% CI)	0.74 (-1.00 to 3.10)	21.9	
<i>Partial regression coefficients</i>			
Years of follow-up, +1 year	0.27 $\pm$ 0.11	0.94	0.011
<i>Baseline risk factors</i>			
Baseline PWV, +2 m/s	-0.71 $\pm$ 0.088	7.83	< 0.0001
Age, +10 years	0.32 $\pm$ 0.052	5.28	<0.0001
Heart rate, +10 bpm	0.18 $\pm$ 0.075	0.79	0.017
Pulse pressure, +15 mm Hg	0.47 $\pm$ 0.079	5.40	<0.0001
History of diabetes mellitus	0.73 $\pm$ 0.31	1.46	0.020
<i>Change in risk factors</i>			
$\Delta$ Heart rate, +10 bpm	0.23 $\pm$ 0.089	0.45	0.011

We performed forward stepwise multiple regression to assess the independent correlations between 4.7 year change in pulse wave velocity and baseline risk factors such as sex, age, body mass index, heart rate, pulse pressure, mean arterial pressure, smoking, history of diabetes mellitus, history of coronary heart disease, serum creatinine, total cholesterol, blood glucose, serum insulin, HOMA-IR, and starting, remaining or stopping with antihypertensive treatment per drug class. We also included longitudinal changes in these risk factors in the stepwise models. We set the  $P$  values for variables to enter the regression models at 0.15 and selected the variables with a  $P$  value below 0.05. Values are mutually adjusted partial regression coefficients ( $\beta$ )  $\pm$  standard error (SE). \*Both baseline and follow-up measurements of PWV were available in 420 subjects. PWV indicates pulse wave velocity;  $R^2$ , additional variance explained by partial regression coefficient.

**Figure S1. Flow Chart for Participants in the FLEMENGHO Study.** Flow diagram shows the progress through the two phases of the longitudinal population study. FLEMENGHO indicates Flemish Study on Environment, Genes and Health Outcomes.

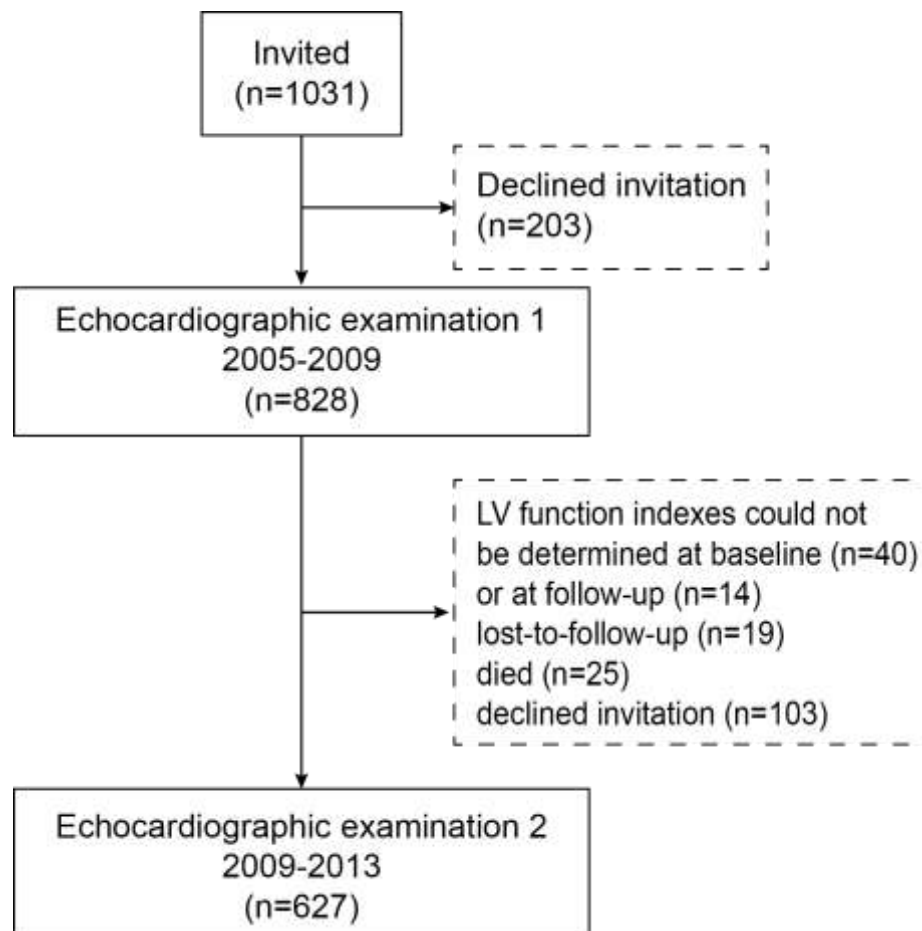
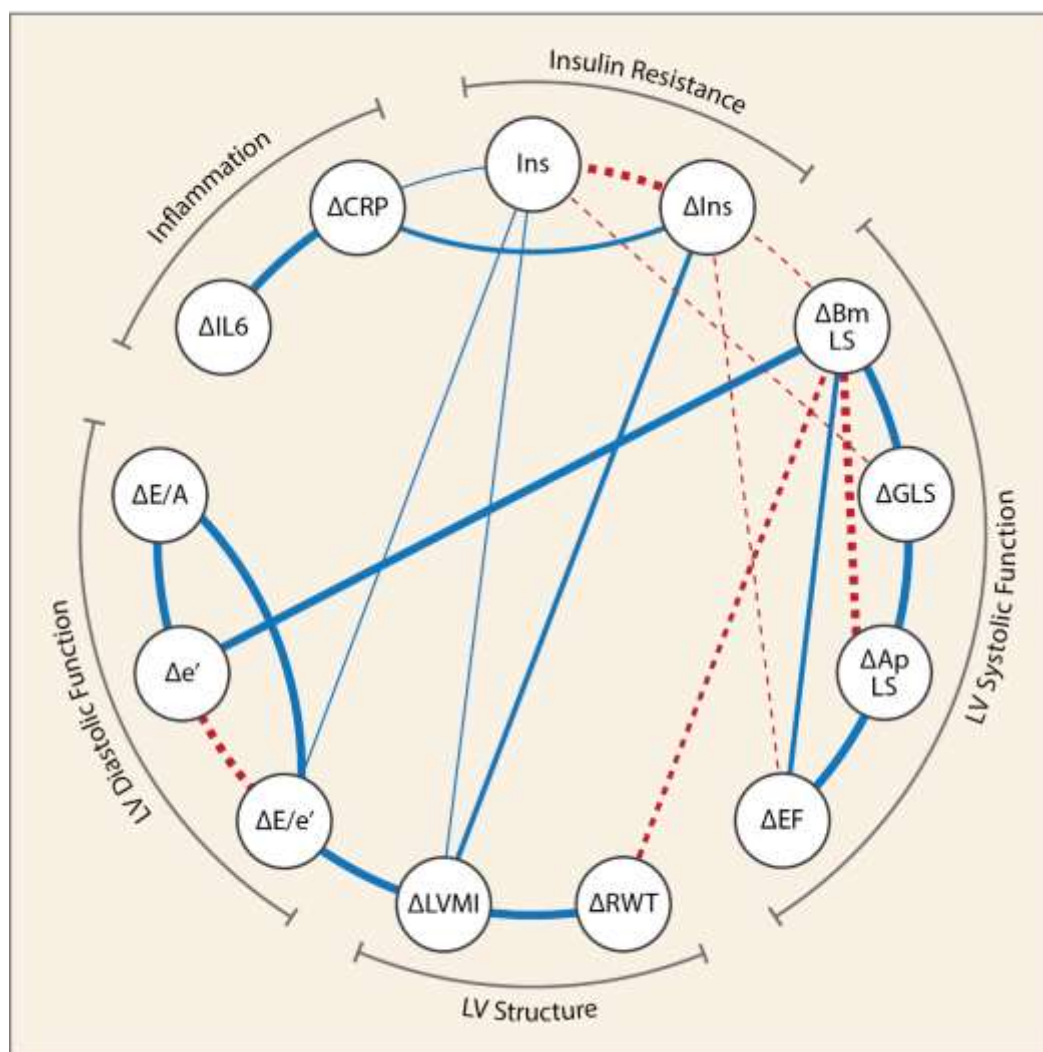




**Figure S2. Partial Correlation Diagram between 4.7 Years Change ( $\Delta$ ) in LV Structure and Function, Inflammatory Markers and Serum Insulin.** The full and dashed lines represent direct and inverse correlations, respectively ( $P < 0.05$  for all). Thicker lines imply stronger relationships. LV changes were adjusted as explained in a footnote to Table 3. ApLS indicates apical longitudinal strain; BmLS, basal-mid longitudinal strain; EF, ejection fraction; GLS, global longitudinal strain; hs-CRP, high-sensitivity C-reactive protein; hs-IL6, high-sensitivity interleukin 6; Ins, insulin; LV, left ventricular; LVMI, LV mass index; RWT, relative wall thickness.



## **Relation of Insulin Resistance to Longitudinal Changes in Left Ventricular Structure and Function in a General Population**

Nicholas Cauwenberghs, Judita Knez, Lutgarde Thijs, Francois Haddad, Thomas Vanassche, Wen-Yi Yang, Fang-Fei Wei, Jan A. Staessen and Tatiana Kuznetsova

*J Am Heart Assoc.* 2018;7:e008315; originally published March 24, 2018;

doi: 10.1161/JAHA.117.008315

The *Journal of the American Heart Association* is published by the American Heart Association, 7272 Greenville Avenue, Dallas, TX 75231  
Online ISSN: 2047-9980

The online version of this article, along with updated information and services, is located on the World Wide Web at:

<http://jaha.ahajournals.org/content/7/7/e008315>